C-glucosidic ellagitannins and galloylated glucoses as potential functional food ingredients with anti-diabetic properties: a study of α-glucosidase and α-amylase inhibition

Nunzio Cardullo[a], Vera Muccilli[a,*], Luana Pulvirenti[a], Anaëlle Cornu[b], Laurent Pouységu[b], Denis Deffieux[b], Stéphane Quideau[b,c], Corrado Tringali[a]

[a] *Dipartimento di Scienze Chimiche, Università degli Studi di Catania, Viale A. Doria 6, 95125-Catania, Italy*

[b] *Univ. Bordeaux, Institut des Sciences Moléculaires (UMR-CNRS 5255), 351 cours de la Libération, 33405 Talence Cedex, France*

[c] *Institut Universitaire de France, 1 rue Descartes, 75231 Paris Cedex 05, France*

Corresponding Author

*(V. M.) Mail: Dipartimento di Scienze Chimiche, Università degli Studi di Catania, V.le A. Doria 6, 95125 Catania, Italy. E-mail: v.muccilli@unict.it. Phone: +39-095-7385041 Fax: +39-095-580138.

Authors e-mails

Nunzio Cardullo, ncardullo@unict.it; Anaëlle Cornu, anaelle.cornu@u-bordeaux.fr; Denis Deffieux, denis.deffieux@u-bordeaux.fr; Laurent Pouységu, laurent.pouysegu@u-bordeaux.fr; Luana Pulvirenti, luanapulvirenti@unict.it; Stéphane Quideau, stephane.quideau@u-bordeaux.fr; Corrado Tringali, ctringali@unict.it

Abstract

Diabetes mellitus is a metabolic disorder characterized by hyperglycemia, which can be counteracted by inhibition of α-glucosidase and α-amylase, both involved in the carbohydrate metabolism. Fourteen *C*-glucosidic ellagitannins and three galloylated glucoses were studied as potential α-glucosidase and α-amylase inhibitors. Most of the compounds were found to be moderate inhibitors of α-amylase, but potent inhibitors of α-glucosidase, showing low-micromolar IC_{50} values, far lower than that of the antidiabetic drug acarbose. This selectivity can be an advantage for their possible application as functional food ingredients with anti-diabetic properties because strong α-amylase inhibition generally causes undesired side effects. The best inhibitors were selected for further studies. Intrinsic fluorescence measurements confirmed their high affinity towards α-glucosidase, highlighting a static quenching mechanism. Circular dichroism measurements and kinetics of inhibition indicated that the most active *C*-glucosidic ellagitannin roburin D (**RobD**) is a competitive inhibitor, whereas α-pentagalloylglucose (**α-PGG**) acts as a mixed-type inhibitor.

Keywords: Hydrolyzable tannins, hypoglycemic activity, α-glucosidase inhibition, α-amylase inhibition, intrinsic fluorescence, inhibition kinetics

1. Introduction

Diabetes mellitus (DM) is a rapidly growing metabolic disorder characterized by insulin hormone dysfunction, and as a result, by high blood glucose levels. Type 2 diabetes (non-insulin-dependent), most frequent in adults, accounts for around 90% of all cases of diabetes. The glycemic control is crucial in patients with DM disease; postprandial hyperglycemia may increase the risk of type 2 diabetes and subsequent complications, such as cardiovascular disease, nephropathy, neuropathy, angiopathy and others (Zheng, Ley, & Hu, 2018). Furthermore, hyperglycemia increases the production of reactive oxygen species, causing oxidative tissue damage (Fiorentino, Prioletta, Zuo, & Folli, 2013). One of the strategies to manage the resulting hyperglycemia is the inhibition of carbohydrate hydrolyzing enzymes, such as α-amylase and α-glucosidase, both involved in the breakdown of dietary carbohydrates (Hakamata, Kurihara, Okuda, Nishio, & Oku, 2009). Acarbose, miglitol and voglibose are currently employed antidiabetic drugs based on carbohydrate structure, able to inhibit both α-amylase and α-glucosidase, thus reducing carbohydrate hydrolysis and consequently glucose absorption. Nevertheless, some undesired side effects, such as flatulence, diarrhea, abdominal and liver disorders, have been reported for acarbose (Godbout & Chiasson, 2007) and similar drugs. Thus, the search for new α-glucosidase and/or α-amylase inhibitors with minor or absent undesired effects is of great importance for DM management. In recent years, natural products were found to be a promising source of α-glucosidase and/or α-amylase inhibitors (Brown, Anderson, Racicot, Pilkenton, & Apostolidis, 2017), thus inspiring the synthesis of new potential antidiabetic agents. Among natural products, some polyphenols occurring in edible plants show α-glucosidase inhibitory activity are attractive as hypoglycemic agents in consideration of their antioxidant properties, which are able to reduce the oxidative damage associated with diabetes complications (Fiorentino et al., 2013). In this framework, some natural product analogues, namely stilbenoid glycosides (Cardullo, Spatafora, Musso, Barresi, Condorelli, & Tringali, 2015), bisphenol neolignans (Pulvirenti, Muccilli, Cardullo, Spatafora, & Tringali, 2017), and rosmarinic acid amides

(Cardullo et al., 2019) were also evaluated as α-glucosidase inhibitors. Among plant polyphenols with antidiabetic properties, tannins raise considerable interest. This group of natural products includes structurally complex plant phenolics that can reach high molecular masses, widely distributed in higher plants, and found in almost all plant foods and beverages. Tannins have attracted scientific interest for their promising biological properties, including antioxidant, antimicrobial, antitumor and antidiabetic activity (Ajebli & Eddouks, 2019; Goncalves, Mateus, & de Freitas, 2011; Serrano, Puupponen-Pimia, Dauer, Aura, & Saura-Calixto, 2009). Considering their structural features, tannins can be classified into three major groups: 1) condensed tannins, 2) hydrolyzable tannins (mainly ellagitannins and gallotannins), and 3) phlorotannins (Quideau, Deffieux, Douat-Casassus, & Pouysegu, 2011). In recent years, the α-glucosidase and/or α-amylase inhibitory activity of ellagi- and gallotannins isolated from different sources have been reported (Ma et al., 2015; Serrano et al., 2009). In this context, commercial tannin mixtures employed in oenology have been recently examined, obtaining fractions enriched in hydrolyzable tannins with high antioxidative capacity and/or α-glucosidase inhibitory activity (Cardullo, Muccilli, Saletti, Giovando, & Tringali, 2018; Muccilli, Cardullo, Spatafora, Cunsolo, & Tringali, 2017; Spinaci, Bucci, Muccilli, Cardullo, Nerozzi, & Galeati, 2019; Spinaci et al., 2018). Tannins are also reported as inhibitors of formation of advanced glycation end-products that contribute to the development and progression of diabetes (Khangholi, Majid, Berwary, Ahmad & Aziz, 2016). All of these findings highlight that tannins found in food and beverages may have a relevant role in the prevention or treatment of DM pathologies, mostly considering their low or absent toxicity. They could also be exploited as components of functional food ingredients with antidiabetic properties. Nevertheless, the difficulty in obtaining tannin samples with satisfactory purity causes a scarcity of systematic studies on the inhibitory properties of individual tannins towards enzymes involved in glucose absorption. Moreover, the search of potential antidiabetic agents from natural sources is frequently limited to the evaluation of α-glucosidase inhibitory activity, since this enzyme

inhibition is part of an established protocol for diabetes therapy and corresponds to the assay most frequently employed in the preliminary steps of the search for new antidiabetic drugs. Thus, the present study is aimed at improving the understanding on the antidiabetic properties of pure *C*-glucosidic ellagitannins and galloylated glucoses through a study of *in vitro* inhibitory effect both on α-glucosidase and α-amylase by using a combination of UV-Vis absorption, fluorescence, circular dichroism and enzyme kinetic analysis.

2. Materials and methods

2.1. Samples and chemicals

Fourteen *C*-glucosidic ellagitannins, namely castalagin (**CSG**), vescalagin (**VSG**), castalin (**CSN**), vescalin (**VSN**), vescalene (**VSE**), roburins A-E (**RobA**-**RobE**), grandinin (**GRA**), acutissimin A (**AcuA**), acutissimin B (**AcuB**), epiacutissimin B (**EAcuB**), and three galloylated glucoses, namely β-glucogallin (**β-GGa**), β-pentagalloylglucose (**β-PGG**), α-pentagalloylglucose (**α-PGG**), were either extracted and purified from natural sources or generated by chemical (hemi)synthesis. **CSG**, **VSG**, **RobA**-**RobE** and **GRA** were extracted and purified from oak heartwood according to previously described protocols (Quideau et al., 2004; Vilhelmova-Ilieva, Jacquet, Quideau, & Galabov, 2014). **CSN**, **VSN** and **VSE** were generated through acidic hydrolytic treatments of **CSG** and **VSN** (Quideau et al., 2005). **AcuA**, **AcuB** and **EAcuB** were produced by hemisynthesis from **VSG** and either catechin or epicatechin as previously described (Quideau et al., 2005; Quideau, Jourdes, Saucier, Glories, Pardon, & Baudry, 2003). **β-GGa**, **β-PGG** and **α-PGG** were produced by total synthesis according to previously described protocols (Sylla, Pouysegu, Da Costa, Deffieux, Monti, & Quideau, 2015). The purity of each compound was assessed by HPLC-UV; detailed data are reported in Supplementary material (Table S1). Quercetin, α-glucosidase from *Saccharomyces cerevisiae* (EC 3.2.1.20, Type I, lyophilized powder, ≥10 units/mg protein; α-GLU), porcine pancreas α-amylase (EC 3.2.1.1, Type VI-B, > 5 units/mg solid;

α-AMY), *p*-nitrophenyl-α-D-glucopyranoside (*p*-NP-α-Glc), starch from potato, 3,5-dinitrosalicylic acid (DNS), sodium potassium tartrate tetrahydrate, acarbose, NaH_2PO_4, Na_2HPO_4 7 H_2O were purchased from Sigma Aldrich. All the chemicals were of analytical purity or higher and distilled water freshly filtered on 0.22 µm was employed in the experiments.

2.2. Measurements of α-glucosidase inhibition

The α-glucosidase inhibition assay was performed using the conditions previously reported (Nunzio Cardullo et al., 2019). Briefly, in a 96-well microplate, the α-glucosidase solution (0.25 U/ml in 50 mM phosphate buffer, pH 6.8; 100 µl) was mixed with different aliquots (2, 4, 6, 8, 10, 15 µl) of tested compounds (stock solutions in methanol ranging from 1.2 mM to 0.6 mM). Then, the substrate *p*NP-α-G (78 µM; 100 µl) was added and the microplate was incubated at 37 °C for 30 min under shaking. The reaction was stopped by adding 1 M Na_2CO_3 solution (10 µl) and the absorbance of *p*NP-α-G was measured at 405 nm with the Synergy H1 microplate reader (BioTek, Bad Friedrichshall, Germany). Acarbose and quercetin were used as reference standards. The assays were performed in triplicate with five different concentrations for each compound. The amount of methanol used in the experiment did not affect the glucosidase inhibitory activity. The inhibition percentage was calculated by the following equation:

$$inhibition\ \% = \frac{(A_{control} - A_{sample})}{A_{control}} * 100 \quad (1)$$

where $A_{control}$ is the absorbance measured for the mixture enzyme/substrate (without tested compounds); A_{sample} is the absorbance measured in the same conditions and in the presence of the tested compounds. The concentration required to inhibit 50% activity of the enzyme (IC_{50}) was calculated by regression analysis.

2.4. Measurements of α-amylase inhibition

The inhibition assay with the α-amylase was performed with slight modifications of a previously reported method (Ali, Houghton, & Soumyanath, 2006). A stock solution of starch

(0.5%) was prepared in 20 mM phosphate buffer (pH 6.9) containing 6.7 mM NaCl, the mixture was stirred at 90 °C for 20 min before use. In a typical experiment, the enzyme solution (6 U/ml in 20 mM phosphate buffer containing 6.7 mM NaCl; 300 µl) was incubated at 37 °C for 10 min with different aliquots (10, 20, 40, 60, 100 µl) of the tested compounds (stock solutions were prepared in water or methanol ranging from 1.2 mM to 0.6 mM). Then, the starch solution (300 µl) was added in the test tubes and the mixtures were incubated at 37 °C for 15 min. The reaction was terminated by the addition of 600 µl of colour reagent solution (96mM DNS with 30% sodium potassium tartrate in 2N NaOH) and the mixtures were heated at 100 °C for 10 min. Each mixture was diluted with water (2 ml) and the absorbance was measured at 540 nm with a Jasco V 750 UV-Vis spectrophotometer (Milan, Italy). For each compound, the assay was performed in triplicate at five different concentrations, acarbose was used as a positive reference. The control, representing 100% enzyme activity, was carried out in the same fashion as for the other experiments, replacing the aliquots of the tested compounds with buffer. The inhibition percentage was calculated by the following equation:

$$inhibition\ \% = \frac{(A_{control} - A_{sample})}{A_{control}} * 100 \quad (2)$$

The concentration required to inhibit 50% activity of the enzyme (IC_{50}) was calculated by regression analysis.

2.5. Fluorescence spectra measurements

The fluorescence spectra of α-glucosidase and α-amylase were recorded on an Agilent Cary Eclipse fluorescence spectrophotometer (Milan, Italy) in the range 300-450 nm, setting the excitation wavelength at 295 nm. Both the slits of excitation and emission were 10 nm. For each tested compound, the experiments (each in triplicate) were performed at 25, 30 and 37 °C; quercetin was employed as a reference compound. The tested compounds did not show fluorescence when irradiated at 295 nm. The concentration of starting solutions of the *C*-glucosidic ellagitannins and

galloylated glucoses were chosen on the basis of the IC_{50} values. In a typical experiment, the α-glucosidase (0.5 µM in 0.1 M phosphate buffer containing 0.1 M NaCl, pH 6.8; 2 ml) or the α-amylase (8.0 µM; 2 ml) was titrated by successive additions of 5 or 10 µl of the tested compounds as follows: for **RobB** and **RobD** from 0 to 2.0 x 10^{-6} mol l^{-1} (curves a → q, Fig. 2A and 2B), for **α-PGG** from 0 to 3.6 x 10^{-6} mol l^{-1} (curves a → z, Fig. 2C), for **RobB** and **RobC** from 0 to 11.0 x 10^{-6} mol l^{-1} (curves a → h, Fig. 2D and 2E). The fluorescence spectrum was acquired 5 min after each addition. The fluorescence measurements were elaborated according to the Stern–Volmer equation (Peng, Zhang, Liao, & Gong, 2016):

$$\frac{F_0}{F} = 1 + K_{sv}[Q] = 1 + K_q\,\tau_0\,[Q] \quad (3)$$

and equation (4) to have information on static quenching.

$$log\,\frac{F_0 - F}{F} = \ logK_a + n\ log[Q] \quad (4)$$

F_0 and F are the fluorescence intensities of enzyme before and after the addition of quencher, respectively; [Q] represents the concentration of quencher (quercetin, **α-PGG**, **RobB**, **RobC**, **RobD**); τ_0 is the average life of the fluorophore without quencher, generally valued about 10^{-8} s (Lakowicz, 2006); K_{SV} and K_q represent the quenching constant and the quenching rate constant, respectively, K_a the binding constant and *n* the number of binding sites.

2.6. CD spectra measurements

CD spectra were recorded on a Jasco J715 spectropolarimeter (Milan, Italy) equipped with a Peltier temperature controller set at 37 °C, and using a 1.0 mm path length quartz cuvette. CD measurements were performed in the range 190-250 nm, in the presence or absence of the tested compounds. Briefly, in each experiment, the α-glucosidase (1 µM in 100 mM phosphate buffer, pH 6.8; 250 µl) was titrated with aliquots (1 or 2 µl) of **RobD** (0.27 mM) or **α-PGG** (0.35 mM), thus the concentration of tested compounds was increased from 0:1 to 4:1 for **RobD** and from 0:1 to 6:1 for **α-PGG**. The spectra were collected after each addition and corrected by subtraction of the blank (100 mM phosphate buffer). CD spectra of **RobD** and **α-PGG**, at the highest concentration tested,

were acquired under the same conditions. The changes of secondary structures of α-glucosidase were estimated with the DichroWeb program (Whitmore & Wallace, 2004, 2008).

2.6. Kinetics of α-glucosidase inhibition

The modes of inhibition of α-glucosidase by **RobB**, **RobD** and **α-PGG** were determined by Lineweaver-Burk plots. The experiments to determine the Michaelis-Menten constant (K_m) and the maximal velocity (v_{max}) were carried out in 96-well microplates (final volume 200 µl), employing a fixed concentration of the enzyme (3.3 mM; 5 µl) and increasing concentrations of *p*NP-α-G (0.15, 0.33, 0.50, 0.80, 1.00, 1.25, 1.50, and 2.00 mM in 50 mM phosphate buffer, pH 6.8) in the absence or presence of the inhibitors. The experiments were carried out in triplicate. The mixtures were incubated at 37 °C and the optical density was read at 405 nm every 1 min for 30 min with the Synergy H1 microplate reader. Optimal amounts of the tested compounds were chosen on the basis of the IC_{50} values.

The inhibition constants were either obtained graphically from secondary plots or were calculated from the following equations:

$$v = \frac{v_{max}S}{K_m\left(1+\frac{I}{K_i}\right)+S} \quad (5)$$

for the competitive inhibitor **RobD**;

$$v = \frac{v_{max}S}{K_m\left(1+\frac{I}{K_i}\right)+S\left(1+\frac{I}{K'_i}\right)} \quad (6)$$

for the mixed-type inhibitor **α-PGG**;

v is the initial velocity in the absence and presence of the inhibitor, S and I are the concentration of substrate and inhibitor, respectively; v_{max} is the maximum velocity, K_m is the Michaelis-Menten constant, K_i is the competitive inhibition constant, and K'_i is the uncompetitive inhibition constant. The replot of slope and Y-intercept of reciprocal plots *versus* the inhibitor concentration gave a straight line, corresponding to K_i and K'_i values, respectively (Meiering et al., 2005).

All the data obtained were compared using Analysis of Variance (ANOVA). P values < 0.05 were considered statistically significant.

3. Results and discussion

3.1. α-Glucosidase and α-amylase inhibitory activity assay.

As mentioned in the Introduction, in many studies carried out searching for antidiabetic agents with negligible side effects, hydrolyzable tannins from different natural sources were identified as α-glucosidase and/or α-amylase inhibitors. However, these reported data seldom referred to purified tannins and the study of enzyme interaction or inhibition mechanism is rarely carried out. Thus, in this work, fourteen ellagitannins (**CSG**, **VSG**, **CSN**, **VSN**, **VSE**, **RobA-E**, **GRA**, **AcuA**, **AcuB**, **EAcuB**) and three galloylated glucoses (**β-GGa**, **β-PGG**, **α-PGG)** listed in Material and Methods, the structures of which are displayed in Fig. 1, were examined for α-glucosidase and α-amylase inhibition.

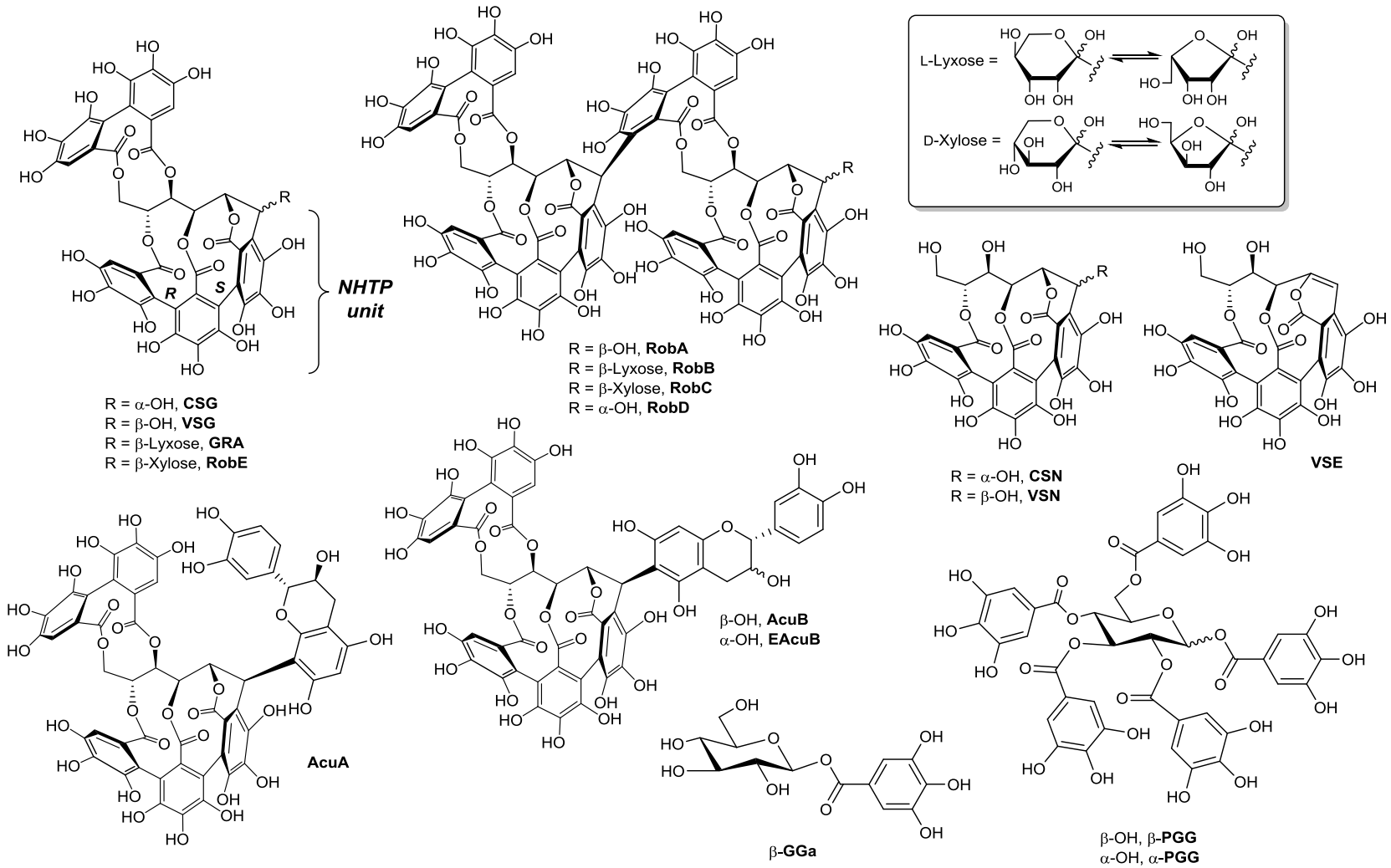

209

210 **Fig.1.** Chemical structures of the *C*-glucosidic ellagitannins and galloylated glucoses tested herein. NB: the representation of the atropoisomerism of
211 the nonahydroxytriphenoyl (NHTP) units of the ellagitannins is depicted throughout this Figure according to the structural revision recently reported
212 by Matsuo and co-workers for vescalagin (**VSG**) and castalagin (**CSG**) (Matsuo, Wakamatsu, Omar, & Tanaka, 2015; Richieu, Peixoto, Pouysegu,
213 Deffieux, & Quideau, 2017).

All of these *C*-glucosidic ellagitannins and galloylated glucoses were subjected to *in vitro* enzymatic activity assays towards yeast α-glucosidase (α-GLU) and porcine pancreatic α-amylase (α-AMY), employing previously reported spectrophotometric methods (Ali et al., 2006; Cardullo et al., 2018). The inhibitory activity data for both α-GLU and α-AMY are reported in Table 1 as the concentration inhibiting 50% of the enzyme activity (IC_{50}, μM); the antidiabetic drug acarbose and the natural flavonoid quercetin were used in the assays as reference standards.

Table 1
α-Glucosidase (α-GLU) and α-amylase (α-AMY) inhibition activity of ellagitannins and galloylated glucoses.

Acronym[a]	IC_{50} ± SD (μM)	
	α-GLU	α-AMY
AcuA	5.7 ± 1.6	101.9 ± 18.7
AcuB	5.0 ± 1.5	166.5 ± 16.7
EAcuB	5.8 ± 1.0	248.0 ± 23.7
GRA	8.9 ± 1.8	412.3 ± 23.7
RobA	5.4 ± 0.9	36.2 ± 4.1
RobB	3.5 ± 0.2	15.6 ± 2.0
RobC	10.9 ± 1.6	8.7 ± 0.9
RobD	2.6 ± 0.2	88.5 ± 9.1
RobE	7.4 ± 2.1	97.9 ± 6.4
VSN	n. i.[b]	n. i.[b]
CSN	n. i.[b]	n. i.[b]
VSE	14.4 ± 0.8	84.7 ± 7.2
VSG	7.2 ± 2.3	89.7 ± 9.3
CSG	7.3 ± 1.6	100.9 ± 11.2
β-GGa	n. i.[b]	n. i.[b]
α-PGG	1.2 ± 0.3	32.9 ± 1.8
β-PGG	1.4 ± 0.2	17.2 ± 1.6
Que	16.4 ± 1.3	33.7 ± 1.6
Aca	260.5 ± 15.2	50.2 ± 4.2

[a] A list of the compound names with their acronyms is given in Materials and Methods (Table S1)
[b] No inhibition observed up to 500 μM

The large majority of the tested compounds strongly inhibited α-GLU with IC_{50} values in the approximate range 1 – 10 μM, lower than that of quercetin (16.4 μM), and proved to be far more potent than acarbose (260.5 μM). The observed inhibition of α-AMY is generally weaker, with only four compounds showing IC_{50} in the range 8.7 – 32.9 μM, all four being more active than quercetin (33.7 μM) and acarbose (50.2 μM). This is paradoxically a positive result, because a strong inhibition of α-AMY is generally associated with undesired side effects, and a correct therapeutic approach should be based on a potent α-GLU inhibition associated with a moderate α-AMY inhibition (Costamagna et al., 2016; Ranilla, Kwon, Apostolidis, & Shetty, 2010). Only three compounds, namely **VSN**, **CSN**, and **β-GGa** showed no inhibition towards both enzymes up to 500 μM. Interestingly, these compounds have both lower molecular masses and a fewer number of phenolic groups than all of the other compounds examined, except the olefinic **VSE**, closely related to the benzylic alcohols **VSN** and **CSN**; this suggests that a more complex polyphenolic structure would be associated with stronger inhibition, at least towards α-GLU. In particular, the effective α-GLU inhibitors **VSG** and **CSG** (IC_{50} = 7.2, 7.3 μM, respectively) differ from the inactive **VSN** and **CSN** by the presence of a hexahydroxydiphenoyl unit at the 4-*O*- and 6-*O*-glucose positions. Apart from that, looking at the structures of the compounds evaluated in this study, no obvious structure-activity relationship can be highlighted, except that the epimeric pentagalloylglucoses **α-PGG** and **β-PGG**, showing IC_{50} values of 1.2 μM and 1.4 μM, are markedly more potent inhibitors of α-GLU than all of the ellagitannins. IC_{50} values in the low micromolar range (2.6 – 10.9 μM) were obtained for the complex flavano-ellagitannins **AcuA**, **AcuB**, and **EAcuB**, as well as for the dimeric *C*-glucosidic ellagitannins **RobA**, **RobB**, **RobC** and **RobD**, the latter being the most potent ellagitannin inhibiting α-GLU. Comparable IC_{50} values towards α-GLU were obtained for the epimeric couples **AcuB**/**EAcuB** (5.0/5.8 μM), **VSG**/**CSG** (7.2/7.3 μM) and **GRA**/**RobE** (8.9/7.4 μM), but this is not confirmed for the epimers **RobA**/**RobD** (5.4/2.6 μM), and **RobB**/**RobC** (3.5/10.9 μM).

The most effective inhibitors of α-AMY are **RobC**, **RobB**, **α-PGG** and **β-PGG** (IC_{50} in the range 8.7 – 32.9 μM), whilst also being potent inhibitors of α-GLU. The ellagitannins **AcuA**, **AcuB**, **EAcuB**, **GRA** and **CSG** are effective inhibitors of α-GLU, but they are only mild inhibitors of α-AMY (IC_{50} in the range 100.9 – 412.3 μM). Analogously, **RobD**, **RobE**, **VSE**, and **VSG**, good or very good inhibitors of α-GLU, are only moderate inhibitors of α-AMY (IC_{50} in the range 84.7 – 89.7 μM). Based on these results, the ellagitannins **RobB** and **RobD**, as well as the pentagalloylated glucose **α-PGG**, potent inhibitors of α-GLU, were selected for a deeper evaluation of the interaction with this enzyme, based on intrinsic fluorescence measurements. Analogously, **RobB** and **RobC**, the most effective inhibitors of α-AMY, were evaluated for the interaction with this enzyme. The pentagalloylated glucose **β-PGG**, epimer of **α-PGG**, was not included in this step because its inhibitory effect on both α-GLU and α-AMY is well documented, and our results are in agreement with literature data (Gyemant et al., 2009; Toda, Kawabata, & Kasai, 2001).

3.2. Fluorescence spectra measurements

The interaction between the selected compounds and α-GLU or α-AMY was investigated by fluorescence quenching experiments. In a protein, tryptophan (Trp) is the main amino acid able to emit fluorescence. The interaction between the enzyme and the substrate modifies the microenvironment of Trp residues, thus producing a decrease in fluorescence (Li, Gao, Shan, Bian, & Zhao, 2009).

More specifically, α-GLU displays an intrinsic fluorescence emission peak near 340 nm when excited at 295 nm; analogously, α-AMY shows an emission peak at near 345 nm when excited at 295 nm. In Figures 2A-C the fluorescence spectra of α-GLU in presence of increasing concentrations of **RobB**, **RobD** and **α-PGG**, respectively, are reported, whereas Figures 2D and 2E show the spectra of α-AMY in presence of increasing concentrations of **RobB** or **RobC**.

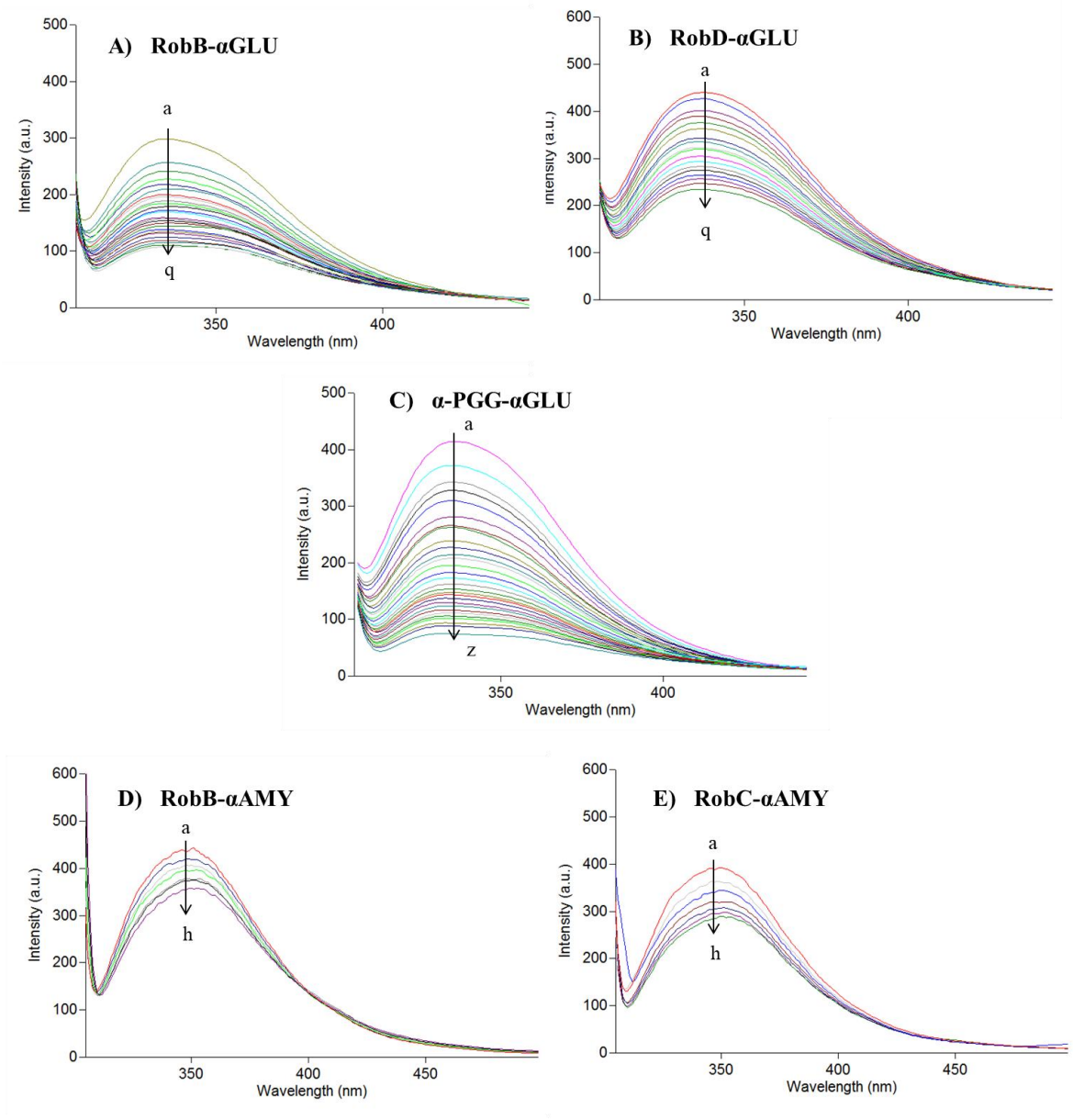

279

280 **Fig. 2.** Fluorescence spectra of α-GLU in the presence of different concentrations of: A) **RobB**, B)
281 **RobD**, C) **α-PGG**. Fluorescence spectra of α-AMY in the presence of different concentrations of :
282 D) **RobB**, E) **RobC**.
283
284 In all the experiments, the fluorescence intensity of both α-GLU and α-AMY was progressively
285 lowered by adding increasing amounts of the tested compounds, thus giving direct evidence of the
286 interaction between these molecules and the enzyme. The experiments were performed at three
287 different temperatures, namely at 25, 30 and 37 °C (See Figure S1 in Supplementary material for
288 experiments carried out at 30 and 37 °C), in order to have some information on the mechanism of
289 quenching. Fluorescence quenching occurs mainly through a static or dynamic mechanism: the

former implies the formation of a non-fluorescent complex, whereas the latter occurs through energy-transfer collisional processes causing the fluorescence quenching (Eftink & Ghiron, 1981). The static mechanism is characterized by a lowering of quenching constant values (K_{sv}) with increasing temperatures because the non-fluorescent complex formation is progressively reduced. Furthermore, in these processes, the rate constant K_q is much higher than 2.0 x 10^{10} l mol^{-1} s^{-1} (Li, Zhou, Gao, Bian, & Shan, 2009). Conversely, in dynamic quenching a temperature increase causes an increasing number of collisions with the consequent raising of K_{SV} values, and K_q is lower than 2.0 x 10^{10} l mol^{-1} s^{-1}.

The K_{SV} and K_q values for **RobB**, **RobC**, **RobD** and **α-PGG** were achieved by linear plots of the Stern-Volmer equation (eq. 3), reporting F_0/F vs [Q]. In Table 2, the K_{sv} and K_q values obtained by plotting F_0/F vs [Q] are reported. As it is evident from these data, for all the tested compounds, the K_{sv} values decrease with increasing temperature (25, 30 and 37 °C), and the resulting K_q values are three order of magnitude greater than 2.0 x 10^{10}, strongly indicating that fluorescence quenching occurs by static mechanism (Peng et al., 2016). In Table 2, we also report the K_{sv} and K_q values obtained for the interaction of quercetin (Que) with α-GLU or α-AMY; these data are in perfect agreement with those previously reported in analogous experiments by other authors (Li et al., 2009; Li et al., 2009).

Further parameters useful to study enzyme-tannin interactions, namely the binding constant (K_a) and the number of binding sites per enzyme molecule (n) were obtained using eq. (4) and are reported in Table 2. It is evident that K_a values are inversely correlated with the temperature, in accordance with the variation of K_{SV}, and this corroborates the above assumption of a static quenching mechanism. Moreover, the K_a values determined for α-GLU were in the order of 10^5 l mol^{-1} for **RobB** and **RobD** and even 10^6 l mol^{-1} for **α-PGG**, suggesting a higher affinity between this pentagalloyglucose and α-GLU, in accordance with a lower IC_{50} value (1.2 μM) in respect to those obtained for the ellagitannins **RobB** (3.5 μM) and **RobD** (2.6 μM). The K_a values obtained for the interaction of **RobB** and **RobC** with α-AMY were respectively in the order of magnitude 10^4

316 and 10^5 l mol^{-1}, suggesting the strongest affinity of **RobC** with the enzyme; also these data are in
317 agreement with the observed IC_{50} values of roburins (Table 1). Furthermore, the number of binding
318 sites *n* was close to 1 for all the tested compounds, indicating that, in our experiments, fluorophore
319 and quencher can form a one-to-one complex, excluding a possible interaction by cooperativity
320 (Lissi, Calderon, & Campos, 2013).

321

322 **Table 2**
323 Quenching constants K_{SV}, quenching rate constants K_q and binding constants K_a of the interaction of
324 **RobB**, **RobC**, **RobD** and **α-PGG** with the proper enzyme.

molecule	T (°C)	K_{SV} (x 10^5 l mol^{-1})	K_q (x10^{13} l mol^{-1})	R^2	K_a (x10^5 l mol^{-1})	n	R^2
			α-glucosidase				
	25	0.97 ± 0.01	0.97 ± 0.01	0.996	1.98 ± 0.01	0.99	0.994
Que	30	0.92 ± 0.01	0.92 ± 0.01	0.993	1.55 ± 0.03	1.03	0.995
	37	0.91 ± 0.01	0.91 ± 0.01	0.996	1.33 ± 0.02	1.06	0.992
	25	6.52 ± 0.03	6.52 ± 0.03	0.995	9.18 ± 0.04	0.87	0.997
RobB	30	5.78 ± 0.02	5.78 ± 0.02	0.995	6.48 ± 0.07	1.00	0.992
	37	5.41 ± 0.02	5.41 ± 0.02	0.998	1.26 ± 0.02	1.04	0.999
	25	4.15 ± 0.01	4.15 ± 0.01	0.998	9.55 ± 0.07	0.91	0.998
RobD	30	4.00 ± 0.03	4.00 ± 0.03	0.998	2.34 ± 0.05	0.95	0.997
	37	3.92 ± 0.02	3.92 ± 0.02	0.997	1.27 ± 0.03	1.06	0.993
	25	9.80 ± 0.04	9.80 ± 0.04	0.995	87.47 ± 0.12	1.09	0.996
α-PGG	30	9.52 ± 0.02	9.52 ± 0.02	0.990	50.11 ± 0.16	1.10	0.994
	37	8.84 ± 0.03	8.84 ± 0.03	0.998	27.33 ± 0.08	1.12	0.996
			α-amylase				
	25	0.46 ± 0.01	0.46 ± 0.01	0.999	1.38 ± 0.05	0.98	0.996
Que	30	0.39 ± 0.02	0.39 ± 0.02	0.994	1.24 ± 0.03	0.99	0.992
	37	0.35 ± 0.03	0.35 ± 0.04	0.999	1.15 ± 0.03	1.08	0.997
	25	0.41 ± 0.02	0.41 ± 0.03	0.994	0.66 ± 0.02	0.99	0.996
RobB	30	0.36 ± 0.01	0.36 ± 0.02	0.991	0.59 ± 0.01	1.00	0.998
	37	0.18 ± 0.01	0.18 ± 0.02	0.995	0.41 ± 0.02	1.10	0.999
	25	1.15 ± 0.01	1.15 ± 0.01	0.998	2.25 ± 0.02	0.91	0.995
RobC	30			0.994		1.05	0.997
	37	1.10 ± 0.03	1.10 ± 0.02	0.997	1.33 ± 0.02	1.08	0.998

0.98 ± 0.01	0.98 ± 0.02	1.02 ± 0.03

325

326

327

328

329

330 *3.3. CD spectra measurements*

331 Circular dichroism (CD) spectroscopy is mostly used to provide information on the secondary
332 structure of proteins in solution and, more specifically, in monitoring conformational changes of a
333 given protein in the presence of a ligand (Allahdad, Varidi, Zadmard, & Saboury, 2018; Kayukawa,
334 de Oliveira, Kaspchak, Sanchuki, Igarashi-Mafra, & Mafra, 2019). Thus, to achieve further
335 confirmation of the interaction of selected tannins with α-GLU, we carried out CD measurements of
336 this enzyme in the absence and presence of different aliquots of **RobD** and **α-PGG,** the compounds
337 showing the higher inhibitory activity towards this enzyme. This step of the study was not extended
338 to α-AMY, considering that both *C*-glucosidic ellagitannins and galloylated glucoses showed lower
339 inhibitory activity and weaker affinity for this enzyme.

340 CD Spectra of α-GLU in the presence of **RobD** or **α-PGG** were acquired in the range 195-250 nm
341 and are reported respectively in Figures 3A and 3B.

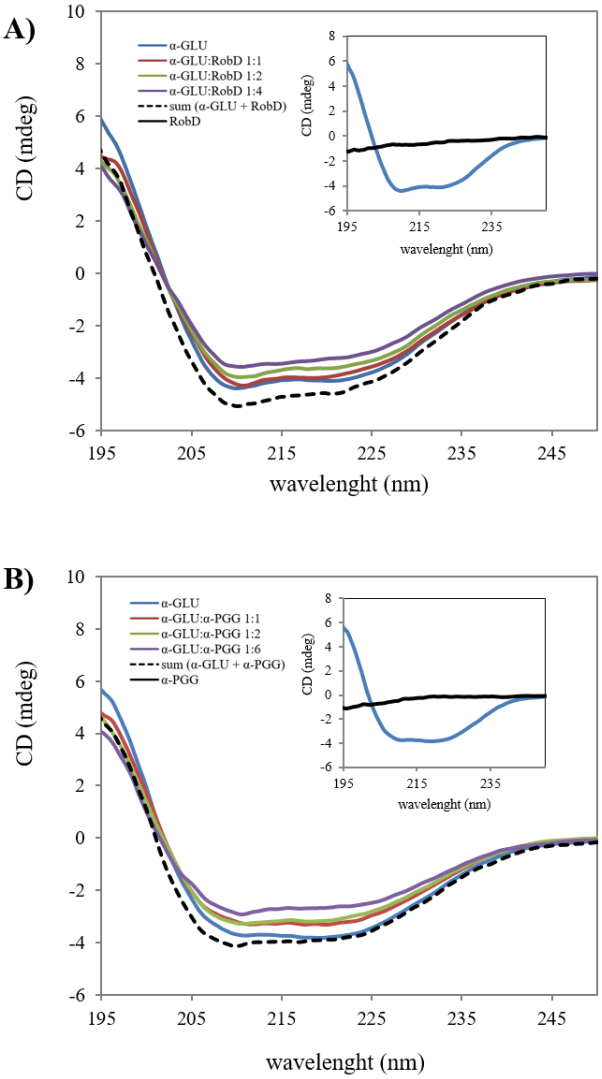

Fig.3.
CD spectra of α-glucosidase (c = 1 x 10^{-6} mol l^{-1}) in the presence of increasing amounts of: A) **RobD**, B) **α-PGG**. Dashed black line corresponds to the algebraic sum of the individual spectra. Insets: spectra of the α-GLU (blue line) and **Rob D**/ **α-PGG** alone (black line).

The CD spectrum of α-GLU shows two negative bands around 210 and 222 nm, attributable to n→π* transition for the peptide bond of α-helix structures, in agreement with previously reported findings (Peng et al., 2016). The CD spectra of **RobD** and **α-PGG** in the absence of α-GLU at the highest concentration tested were acquired as well (Figure 3, insets). As shown in Figure 3, the intensity of both bands observed in the spectrum of α-GLU decreases by addition of increasing amounts of **RobD** or **α-PGG**, indicating the loss of part of the α-helix structures. This variation in

the secondary structure of the α-GLU could originate from the interaction with **RobD** or **α-PGG**. The CD spectra obtained by titration of the enzyme with increasing amount of ligand show a marked change in spectroscopic signals compared with the theoretical spectra of α-GLU and **Rob D**/ **α-PGG** at the highest concentration tested (Figure 3, dashed black lines), thus suggesting that an enzyme-ligand interaction has occurred.

CD data were further analysed by the DichroWeb program in order to quantify changes in the secondary structure. According to these data (reported in Table S2 in Supplementary material), the interaction between the α-GLU and **RobD** caused a decrease of α-helix content (from 30% to 26% at the highest concentration of inhibitor tested). Analogously, the α-helix content for α-GLU gradually decreased with increasing amounts of **α-PGG (**from 30% to 20% at the highest concentration of inhibitor tested). These findings further support the data obtained by fluorescence measurements. The decrease in α-helix induced by **RobD** and **α-PGG** is in agreement with the same behaviour previously observed for the interaction of other tannin-related compounds with α-glucosidase (Ma et al., 2015).

3.4. Kinetics of α-glucosidase inhibition

As a final step of this research, the kinetic of α-GLU inhibition by **RobD** and **α-PGG** was studied by means of UV spectroscopy and the mode of inhibition was determined by plotting the reciprocal of substrate concentration against the reciprocal of respective product formation rate, thus obtaining the Lineweaver-Burk plots. The obtained values for the kinetic parameters are listed in Table S3 (Supplementary material). As shown in Figure 4A, the data lines of the Lineweaver–Burk plot obtained for **RobD** intersected the y-axes in the first quadrant, indicating that this *C*-glucosidic ellagitannin acts as a competitive inhibitor. Increasing concentration of **RobD** unaffected the V_{max} value (0.40 μM min^{-1}), whereas it increased the K_m value (from 3.03 to 7.88 μM), supporting the finding that **RobD** inhibits the α-GLU activity competitively. Moreover, a dissociation constant (K_i) value of 1.60 μM for the enzyme-inhibitor complex was determined from the slope replot of

Lineweaver–Burk lines *versus* the concentration of **RobD**. As reported in the inset of Figure 4A, the data linearly fitted, suggesting a complete competitive inhibition and confirming that **RobD** bound to the free α-GLU.

The data lines on the Lineweaver–Burk plot obtained for **α-PGG** intersected in the second quadrant, indicating that this pentagalloylglucose acts as a mixed-type inhibitor (Figure 4B). The inhibition caused by **α-PGG** modified both V_{max} (from 0.15 to 0.08 μM min^{-1}) and K_m (from 0.50 to 1.62 μM) values with increasing concentration of inhibitor (Table S3). From the Eq. (6), the dissociation constants K_i, which is related with the formation of an enzyme-inhibitor complex (EI), and K'_i, which is related with the interaction of inhibitor with the enzyme-substrate complex (IES), were calculated. Furthermore, the replots of slope and Y-intercept *versus* **α-PGG** concentration (insets in Figure 4B) were linearly fitted, suggesting for this inhibitor a complete and single inhibition site or a single class of inhibition site on the enzyme (Peng et al., 2016), in agreement with the *n* value obtained by fluorescence measurements. Finally, a K_i value of 0.52 μM and a K'_i value of 2.32 μM were obtained, indicating that **α-PGG** was able to bind more easily to the free α-glucosidase rather than the ES complex.

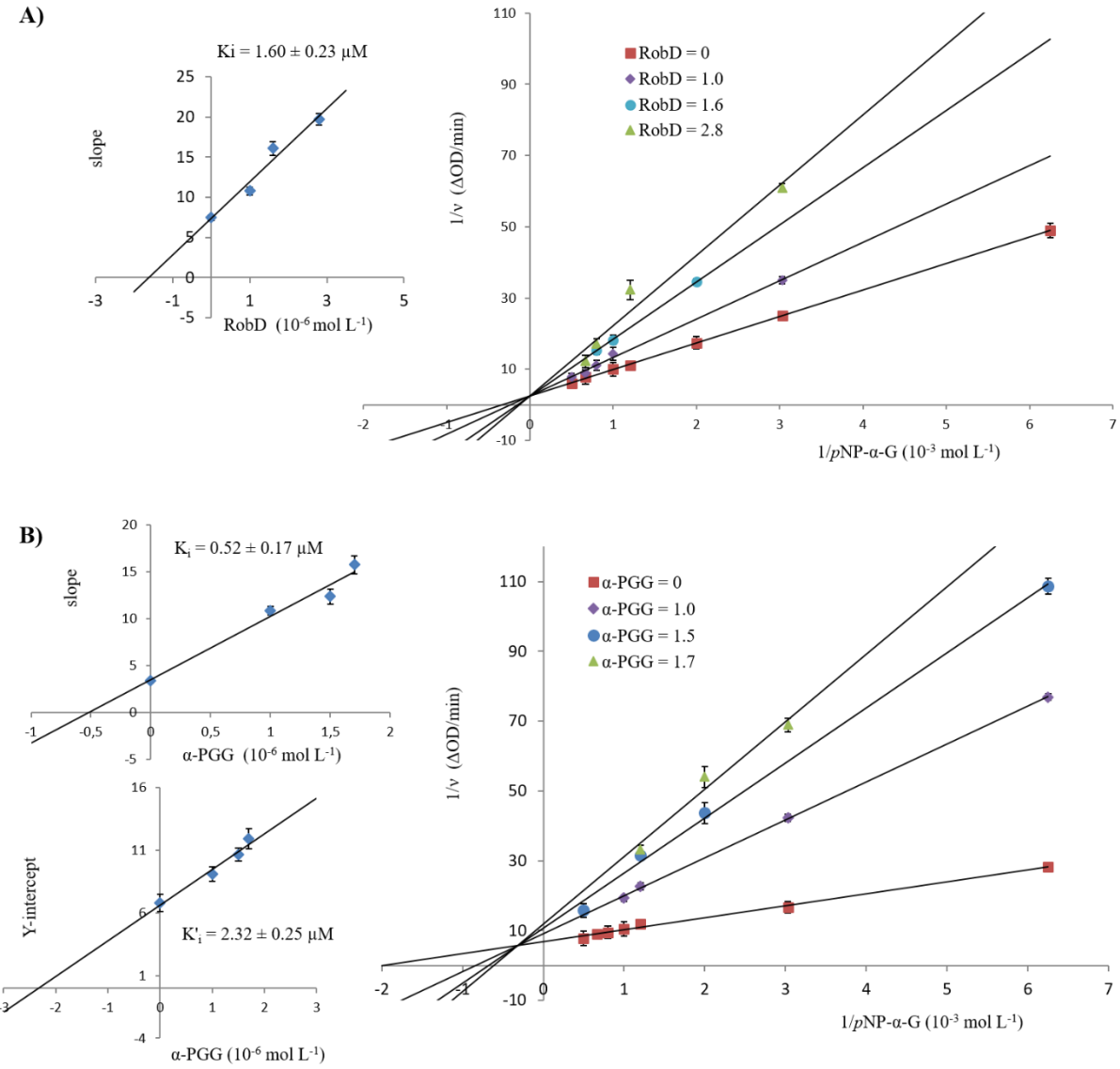

Fig. 4. Lineweaver-Burk plots of α-glucosidase inhibition at different concentrations of substrate (*p*NP-α-G) of: A) **RobD**; B) **α-PGG**. The insets depict the secondary plots of slope and Y-intercept vs inhibitors concentration.

4. Conclusions

In this work, we evaluated as inhibitors of yeast α-glucosidase and porcine pancreatic α-amylase fourteen *C*-glucosidic ellagitannins and three galloylated glucoses. Many compounds were potent inhibitors of α-GLU, showing IC_{50} values less than 10 µM, far lower than that of the antidiabetic drug acarbose (260.5 µM). Conversely, only four compounds significantly inhibited α-

AMY with IC_{50} lower than those of quercetin or acarbose. Since a strong inhibition of α-AMY generally causes undesired side effects, this could be an advantage for possible therapeutic applications. The ellagitannins **RobB** and **RobD**, as well as the galloylated glucose **α-PGG**, the most potent α-GLU inhibitors and moderate to good inhibitors of α-AMY, were selected for a study of the interaction with α-glucosidase, employing fluorescence quenching experiments. Analogously, **RobB** and **RobC** were evaluated for the interaction with α-amylase. The fluorescence experiments confirmed a strong interaction of these tannins with α-GLU; moreover, K_{sv} and K_q values were in agreement with a static quenching mechanism. A similar behaviour was observed for α-AMY. More specifically, the K_a values obtained for α-GLU suggested a higher affinity between **α-PGG** and the enzyme with respect to **RobB** and **RobD**, in agreement with IC_{50} values. Analogously, the K_a value obtained for the interaction of **RobC** with α-AMY was higher than that obtained for **RobB.** Further confirmation of the interaction with α-GLU was obtained through CD spectra measurements, showing that the addition of inhibitors causes a progressive loss of α-helix portions in the structure of the enzyme. As a final step, the kinetics of α-GLU inhibition by **RobD** and **α-PGG** was studied by means of UV spectroscopy. The results of Lineweaver-Burk plots pointed out that the ellagitannin **RobD** is a competitive inhibitor, whereas the pentagalloylglucose **α-PGG** acts as a mixed-type inhibitor.

Overall, the data obtained in this work show that both *C*-glucosidic ellagitannins and certain galloylated glucopyranoses may have a relevant role in the prevention of Diabetes Mellitus and suggest a possible development of their use as functional food ingredients with antidiabetic properties.

Acknowledgements

This research was supported by ‘Piano della Ricerca di Ateneo 2016-2018, Linea d’intervento 2’ of Università degli Studi di Catania, by MIUR ITALY PRIN 2017 (Project No. 2017A95NCJ_003),

by the Ministère de l'Enseignement supérieur, de la Recherche et de l'Innovation and by the Centre National de la Recherche Scientifique (CNRS). The authors acknowledge the Bio-Nanotech Research and Innovation Tower (BRIT) for making available the Synergy H1 microplate reader and Prof. Alessandro D'Urso (University of Catania) for CD spectra acquisition.

References

Ajebli, M., & Eddouks, M. (2019). The Promising Role of Plant Tannins as Bioactive Antidiabetie Agents. *Current Medicinal Chemistry, 26*(25), 4852-4884

Ali, H., Houghton, P. J., & Soumyanath, A. (2006). Alpha-amylase inhibitory activity of some Malaysian plants used to treat diabetes; with particular reference to *Phyllanthus amarus*. *Journal of Ethnopharmacology, 107*(3), 449-455. https://doi.org/10.1016/j.jep.2006.04.004.

Allahdad, Z., Varidi, M., Zadmard, R., & Saboury, A. A. (2018). Spectroscopic and docking studies on the interaction between caseins and beta-carotene. *Food Chemistry, 255*, 187-196. https://doi.org/10.1016/j.foodchem.2018.01.143.

Brown, A., Anderson, D., Racicot, K., Pilkenton, S. J., & Apostolidis, E. (2017). Evaluation of Phenolic Phytochemical Enriched Commercial Plant Extracts on the In Vitro Inhibition of alpha-Glucosidase. *Frontiers in Nutrition, 4*. https://doi.org/10.3389/fnut.2017.00056.

Cardullo, N., Catinella, C., Floresta, G., Muccilli, V., Rosselli, S., Rescifina, A., Bruno, M., & Tringali, C. (2019). Synthesis of Rosmarinic Acid Amides as Antioxidative andHypoglycemic Agents. *Journal of Natural Products*. https://doi.org/10.1021/acs.jnatprod.8b01002.

Cardullo, N., Muccilli, V., Saletti, R., Giovando, S., & Tringali, C. (2018). A mass spectrometry and ^{1}H NMR study of hypoglycemic and antioxidant principles from a *Castanea sativa* tannin employed in oenology. *Food Chemistry, 268*, 585-593. https://doi.org/10.1016/j.foodchem.2018.06.117.

Cardullo, N., Spatafora, C., Musso, N., Barresi, V., Condorelli, D., & Tringali, C. (2015). Resveratrol-Related Polymethoxystilbene Glycosides: Synthesis, Antiproliferative Activity, and Glycosidase Inhibition. *Journal of Natural Products, 78*, 2675-2683.

Costamagna, M. S., Zampini, I. C., Alberto, M. R., Cuello, S., Torres, S., Perez, J., Quispe, C., Schmeda-Hirschmann, G., & Isla M I. (2016). Polyphenols rich fraction from *Geoffroea decorticans* fruits flour affects key enzymes involved in metabolic syndrome, oxidative stress and inflammatory process. *Food Chemistry, 190*, 392-402. https://doi.org/10.1016/j.foodchem.2015.05.068.

Eftink, M. R., & Ghiron, C. A. (1981). Fluorescence quenching studies with proteins. *Analytical Biochemistry, 114*, 199-227.

Fiorentino, T. V., Prioletta, A., Zuo, P., & Folli, F. (2013). Hyperglycemia-induced Oxidative Stress and its Role in Diabetes Mellitus Related Cardiovascular Diseases. *Current Pharmaceutical Design, 19*(32), 5695-5703. https://doi.org/10.2174/1381612811319320005.

Godbout, A., & Chiasson, J.-L. (2007). Who Shold Benefit from the Use of Alpha-Glucosidase Inhibitors. *Current Diabets Reports, 7*, 333-339.

Goncalves, R., Mateus, N., & de Freitas, V. (2011). Inhibition of alpha-amylase activity by condensed tannins. *Food Chemistry*, *125*(2), 665-672. https://doi.org/10.1016/j.foodchem.2010.09.061.

Gyemant, G., Zajacz, A., Becsi, B., Ragunath, C., Ramasubbu, N., Erdodi, F., Batta, G., & Kandra, L. (2009). Evidence for pentagalloyl glucose binding to human salivary alpha-amylase through aromatic amino acid residues. *Biochimica Et Biophysica Acta-Proteins and Proteomics, 1794*(2), 291-296. https://doi.org/10.1016/j.bbapap.2008.10.012.

Hakamata, W., Kurihara, M., Okuda, H., Nishio, T., & Oku, T. (2009). Design and Screening Strategies for alpha-Glucosidase Inhibitors Based on Enzymological Information. *Current Topics in Medicinal Chemistry*, *9*(1), 3-12. https://doi.org/10.2174/156802609787354306.

Kayukawa, C. T. M., de Oliveira, M. A. S., Kaspchak, E., Sanchuki, H. B. S., Igarashi-Mafra, L., & Mafra, M. R. (2019). Effect of tannic acid on the structure and activity of *Kluyveromyces lactis* beta-galactosidase. *Food Chemistry*, *275*, 346-353. https://doi.org/10.1016/j.foodchem.2018.09.107.

Lakowicz, J. R. (2006). *Principles of Fluorescence Spectroscopy*. (3rd edition ed.). New York: Springer.

Li, Y., Gao, F., Shan, F., Bian, J., & Zhao, C. (2009). Study on the Interaction between 3 Flavonoid Compounds and alpha-Amylase by Fluorescence Spectroscopy and Enzymatic Kinetics. *Journal of Food Science*, *74*(3), C199-C203. https://doi.org/10.1111/j.1750-3841.2009.01080.x.

Li, Y. Q., Zhou, F. C., Gao, F., Bian, J. S., & Shan, F. (2009). Comparative Evaluation of Quercetin, Isoquercetin and Rutin as Inhibitors of a-Glucosidase. *57*, 11463–11468. https://doi.org/10.1021/jf903083h

Lissi, E., Calderon, C., & Campos, A. (2013). Evaluation of the Number of Binding Sites in Proteins from their Intrinsic Fluorescence: Limitations and Pitfalls. *Photochemistry and Photobiology*, *89*(6), 1413-1416. https://doi.org/10.1111/php.12112.

Ma, H., Wang, L., Niesen, D. B., Cai, A., Cho, B. P., Tan, W., Gu, Q., Xu, J., & Seeram, N. P. (2015). Structure activity related, mechanistic, and modeling studies of gallotannins containing a glucitol-core and alpha-glucosidase. *Rsc Advances*, *5*(130), 107904-107915. https://doi.org/10.1039/c5ra19014b.

Matsuo, Y., Wakamatsu, H., Omar, M., & Tanaka, T. (2015). Reinvestigation of the Stereochemistry of the *C*-Glycosidic Ellagitannins, Vescalagin and Castalagin. *Organic Letters*, *17*(1), 46-49. https://doi.org/10.1021/ol503212v.

Meiering, S., Inhoff, O., Mies, J., Vincek, A., Garcia, G., Kramer, B., Dormeyer, M., & Krauth-Siegel, R. L. (2005). Inhibitors of *Trypanosoma cruzi* trypanothione reductase revealed by virtual screening and parallel synthesis. *Journal of Medicinal Chemistry*, *48*(15), 4793-4802. https://doi.org/10.1021/jm050027z.

Muccilli, V., Cardullo, N., Spatafora, C., Cunsolo, V., & Tringali, C. (2017). α-Glucosidase inhibition and antioxidant activity of an oenological commercial tannin. Extraction, fractionation and analysis by HPLC/ESI-MS/MS and ^{1}H NMR. *Food Chemistry*, *215*, 50-60. https://doi.org/10.1016/jfoodchem.2016.07.136.

Peng, X., Zhang, G. W., Liao, Y. J., & Gong, D. M. (2016). Inhibitory kinetics and mechanism of kaempferol on alpha-glucosidase. *Food Chemistry*, *190*, 207-215. https://doi.org/10.1016/j.foodchem.2015.05.088.

Pulvirenti, L., Muccilli, V., Cardullo, N., Spatafora, C., & Tringali, C. (2017). Chemoenzymatic Synthesis and alpha-Glucosidase Inhibitory Activity of Dimeric Neolignans Inspired by Magnolol. *Journal of Natural Products*, *80*(5), 1648-1657. https://doi.org/10.1021/acs.jnatprod.7b00250.

Quideau, S., Deffieux, D., Douat-Casassus, C., & Pouysegu, L. (2011). Plant Polyphenols: Chemical Properties, Biological Activities, and Synthesis. *Angewandte Chemie International Edition*, *50*(3), 586-621. https://doi.org/10.1002/anie.201000044.

Quideau, S., Jourdes, M., Lefeuvre, D., Montaudon, D., Saucier, C., Glories, Y., Pardon, P., & Pourquier, P. (2005). The chemistry of wine polyphenolic *C*-glycosidic ellagitannins targeting human topoisomerase II. *Chemistry-A European Journal, 11*(22), 6503-6513. https://doi.org/10.1002/chem.200500428.

Quideau, S., Jourdes, M., Saucier, C., Glories, Y., Pardon, P., & Baudry, C. (2003). DNA topoisomerase inhibitor acutissimin A and other flavano-ellagitannins in red wine. *Angewandte Chemie International Edition, 42*(48), 6012-6014. https://doi.org/10.1002/anie.200352089.

Quideau, S., Varadinova, T., Karagiozova, D., Jourdes, M., Pardon, P., Baudry, C., . Genova, P., Diakov, T., & Petrova, R. (2004). Main structural and stereochemical aspects of the antiherpetic activity of nonahydroxyterphenoyl-containing *C*-glycosidic ellagitannins. *Chemistry & Biodiversity, 1*(2), 247-258. https://doi.org/10.1002/cbdv.200490021.

Ranilla, L. G., Kwon, Y. I., Apostolidis, E., & Shetty, K. (2010). Phenolic compounds, antioxidant activity and *in vitro* inhibitory potential against key enzymes relevant for hyperglycemia and hypertension of commonly used medicinal plants, herbs and spices in Latin America. *Bioresource Technology, 101*(12), 4676-4689. https://doi.org/10.1016/j.biortech.2010.01.093.

Richieu, A., Peixoto, P. A., Pouysegu, L., Deffieux, D., & Quideaeu, S. (2017). Bioinspired Total Synthesis of (–)-Vescalin: A Nonahydroxytriphenoylated C-Glucosidic Ellagitannin. *Angewandte Chemie International Edition, 56*(44), 13833-13837. https://doi.org/10.1002/anie.201707613.

Serrano, J., Puupponen-Pimia, R., Dauer, A., Aura, A. M., & Saura-Calixto, F. (2009). Tannins: Current knowledge of food sources, intake, bioavailability and biological effects. *Molecular Nutrition & Food Research, 53*, S310-S329. https://doi.org/10.1002/mnfr.200900039.

Spinaci, M., Bucci, D., Muccilli, V., Cardullo, N., Nerozzi, C., & Galeati, G. (2019). A polyphenol-rich extract from an oenological oak-derived tannin influences in vitro maturation of porcine oocytes. *Theriogenology, 129*, 82-89. https://doi.org/10.1016/j.theriogenology.2019.02.017.

Spinaci, M., Muccilli, V., Bucci, D., Cardullo, N., Gadani, B., Tringali, C., Tamanini, C., & Galeati, G. (2018). Biological effects of polyphenol-rich extract and fractions from an oenological oak-derived tannin on in vitro swine sperm capacitation and fertilizing ability. *Theriogenology, 108*, 284-290. https://doi.org/10.1016/j.theriogenology.2017.12.015.

Sylla, T., Pouysegu, L., Da Costa, G., Deffieux, D., Monti, J. P., & Quideau, S. (2015). Gallotannins and Tannic Acid: First Chemical Syntheses and In Vitro Inhibitory Activity on Alzheimer's Amyloid-Peptide Aggregation. *Angewandte Chemie International Edition, 54*(28), 8217-8221. https://doi.org/10.1002/anie.201411606.

Toda, M., Kawabata, J., & Kasai, T. (2001). Inhibitory effects of ellagi- and gallotannins on rat intestinal alpha-glucosidase complexes. *Bioscience Biotechnology and Biochemistry, 65*(3), 542-547. https://doi.org/10.1271/bbb.65.542.

Vilhelmova-Ilieva, N., Jacquet, R., Quideau, S., & Galabov, A. S. (2014). Ellagitannins as synergists of ACV on the replication of ACV-resistant strains of HSV 1 and 2. *Antiviral Research, 110*, 104-114. https://doi.org/10.1016/j.antiviral.2014.07.017.

Whitmore, L., & Wallace, B. A. (2004). DICHROWEB, an online server for protein secondary structure analyses from circular dichroism spectroscopic data. *Nucleic Acids Research, 32*, W668-W673. https://doi.org/10.1093/nar/gkh371.

Whitmore, L., & Wallace, B. A. (2008). Protein secondary structure analyses from circular dichroism spectroscopy: Methods and reference databases. *Biopolymers, 89*(5), 392-400. https://doi.org/10.1002/bip.20853.

Zheng, Y., Ley, S. H., & Hu, F. B. (2018). Global aetiology and epidemiology of type 2 diabetes mellitus and its complications. *Nature Reviews Endocrinology, 14*(2), 88-98. https://doi.org/10.1038/nrendo.2017.151.